

## Short Paper

# Visualization of Aerodynamic Noise Source in the Wake of a Rotating Cylinder

Iida, A.\*<sup>1</sup>, Mizuno, A.\*<sup>1</sup>, Brown, R. J.\*<sup>2</sup> and Kato, C.\*<sup>3</sup>

\*1 Department of Mechanical Engineering, Kogakuin University, 2665 Nakano-machi, Hachioji, Tokyo, 192-0015 Japan. E-mail: iida@fluid.mech.kogakuin.ac.jp

\*2 School of Mechanical, Manufacturing and Medical Engineering, Queensland University of Technology, 2434 BRISBANE QLD 4001 Australia.

\*3 Institute of Industrial Science, University of Tokyo, 4-6-1 Komaba, Meguro-ku, Tokyo, 153-8505 Japan.

Received 21 August 2006 and Revised 12 September 2006

## 1. Introduction

The maximum speed of high-speed trains has been in an upward trend for several years. Cooling flow rates inside air conditioners and computers are also increasing. As a result aerodynamic noise radiating from these products is rapidly increasing. This is in part because aerodynamic noise is proportional to the sixth power of flow velocity. The problem of aerodynamic noise in these products therefore must be addressed.

The purpose of this investigation was to develop a method for reducing aerodynamic noise from a cylinder. To control the aerodynamic noise, aerodynamic noise radiated from a rotating cylinder was calculated using a large eddy simulation and Curle's theory (Kato et al., 1994). The sound source distribution was also visualized with Powell's theory (Powell, 1964). These results indicated that the aerodynamic noise can be controlled with rotational speed. Moreover, the noise source distribution shows the contribution of the source term of vorticity and velocity fluctuations.

## 2. Numerical Methods

In order to simulate an unsteady turbulent flow field around a rotating cylinder we used CFD code of FrontFlow/Blue developed by Frontier Simulation Software for Industrial Science.

The governing equations used for the flow field around the rotating cylinder are the continuity equation and incompressible Navier-Stokes equations. The standard Smagorinsky model was adopted as the sub-grid scale model for turbulence. The Van-Driesr wall-damping function was also used for modeling of near-wall effects. The Smagorinsky constant was set at 0.15 and the grid-filler size was computed as the cube-root of the volume of each finite element. The spatial filters of the governing equations were solved by a stream-upwind, second-order finite element formulation (Kato et al., 1994).

The total number of three dimensional finite element meshes was about 400,000. At the upstream boundary of the inlet, a uniform velocity was prescribed. At the downstream boundary, the fluid traction was assumed to be zero (traction free condition). On the cylinder surface, rotational speed or non-slip condition was prescribed to simulate cylinder rotation. Symmetric boundary conditions were used for both sides of the span wise direction. The distance in the span wise direction is equal to 2 times the diameter. To estimate the effect of the rotational speed of the cylinder, the velocity ratio of the rotational speed to the uniform flow,  $\alpha$ , was changed from 0 to 3 and the Reynolds number from  $10^3$  to  $10^4$ . The far field sound pressure radiated from a low-Mach number flow can be calculated from Lighthill-Curle's equation (Kato et al., 1994).

## 3. Results and Discussion

Figure 1 shows the vorticity structure around a cylinder at a Reynolds number of  $10^3$ . In the case of the low velocity ratio, large-scale vorticity structures are observed and the separated shear layers roll up just behind the cylinder. On the other hand, alternative vorticity structures disappear at a high velocity ratio. In the case of  $\alpha = 3.0$ , coherent structure is not observed.

Figure 2 shows the aerodynamic noise from a rotating cylinder with Lighthill-Curle's equation. The predicted noise level does not depend on the Reynolds number, but depends strongly on the

velocity ratio,  $\alpha$  (Fujisawa et al., 2005). When the alternative vorticity structures exist, noise levels increase in comparison to the noise level of a non-rotating cylinder. On the other hand, sound levels decrease at high velocity ratios,  $\alpha > 2.0$ . The aerodynamic noise from a rotating cylinder at  $\alpha = 3.0$  is 10 dB lower than that of the stationary cylinder. This indicates that the rotational speed is one of the controlling factors in aerodynamic noise reduction.

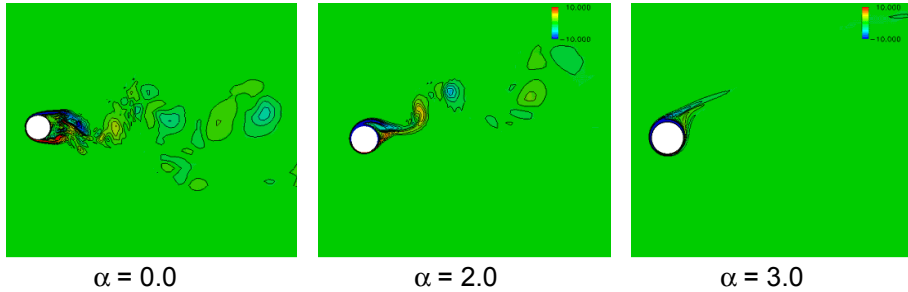


Fig. 1. Distribution of vorticity contours around a rotating cylinder.

According to Powell's theory, aerodynamic noise is caused by the coupling source term  $\omega \times u$ , where  $\omega$  and  $u$  denote vorticity and velocity vector, respectively. Figure 3 shows the source term of the rotating cylinder. In the case of a non-rotating cylinder, the aerodynamic sound source lies just behind the cylinder. In the case of  $\alpha = 2.0$ , the source term decreases due to the effect of the rotation. However, the distribution of the source term is almost the same as for  $\alpha = 0.0$ . Thus the noise level for  $\alpha = 2.0$  is almost the same as the noise level for  $\alpha = 0.0$ . In contrast, the distribution of the sound source is different in the case of  $\alpha = 3.0$ . The sound source only exists around the cylinder surface and the source term is not seen in the wake of the cylinder. The origin of the aerodynamic source comes from the separated shear layers, because the velocity gradient is large at the boundary layer of the cylinder surface. In the case of the rotating cylinder, the velocity gradient is large compared to that of the stationary cylinder. The intensity of the source term due to the separated shear layer is large at the high velocity ratio; however, aerodynamic sound is small at the high velocity ratio. Since the aerodynamic noise is caused by the unsteady vortex motion, the aerodynamic sound generation depends on not only on the source term intensity of the shear layers but also in the source term fluctuation in time and space domains.

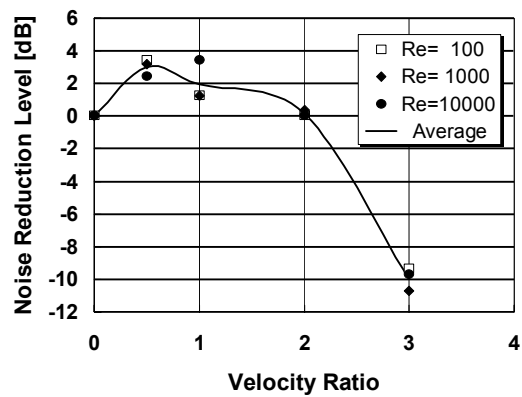


Fig. 2. Noise reduction effect on the velocity ratio of a rotating cylinder.

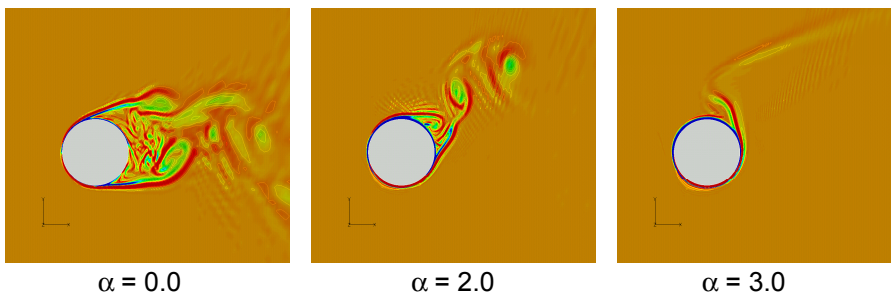


Fig. 3. Distribution of aerodynamic sound source term around a rotating cylinder.

**References**

Kato, C., et al., Numerical Prediction of Aerodynamic Sound by Large Eddy Simulation, Trans. Jpn. Soc. Mech. Eng., 60-569 B (1994), 126-132 (in Japanese).  
 Powell, A., Theory of Vortex Sound, J. Acoustical Society of America, 36 (1964), 177-195.  
 Fujisawa, N., et al., A study on drag reduction of a rotationally oscillating circular cylinder at low Reynolds number, Journal of Visualization, 8-1 (2005), 41-48.